Table III. Rate Constants for the Disappearance of 8a under Various Conditions[a]

k_{obsd},	conditions
$(4.6 \pm 0.3) \times 10^{-5}$ [b]	[8a]:[PPh_3] = 50[d]
$(4.9 \pm 0.8) \times 10^{-5}$ [b]	[8a]:[PPh_3] = 50[d]
$(5.0 \pm 0.3) \times 10^{-5}$ [b]	[8a]:[PPh_3] = 100[d]
$(4.7 \pm 0.2) \times 10^{-5}$ [b]	[8a]:[PPh_3] = 100[e]
$(4.2 \pm 0.2) \times 10^{-3}$ [c]	[8a]:[PPh_3]:[$RP^+Ph_3Cl^-$][f] = 1:1:15[d]
$(3.0 \pm 0.4) \times 10^{-3}$ [c]	[8a]:[PPh_3]:[$RP^+Ph_3Cl^-$][f] = 1:1:20[d]

[a] In 1,2-dichloroethane at 85 °C. [b] k_{obsd} values given in s^{-1}. [c] k_{obsd} values given in M^{-1} s^{-1}. [d] Followed by UV spectroscopy at 330 nm. [e] Followed by IR spectroscopy at 2070 cm^{-1}. [f] [$RP^+Ph_3Cl^-$] = allyltriphenylphosphonium chloride.

an absorbing species. The equation $1/A = kt + 1/A_0$ was used to calculate second-order rate constants with $[\mathbf{8a}]_0 = [PPh_3]_0$. The results are shown in Table III.

Initial Rates. A. A 25-mL two-neck flask with a side arm was charged with 18.9 mg (0.02 mmol) of complex **8a** and 262 mg (1.0 mmol) of triphenylphosphine. After the flask was evacuated and flushed with nitrogen, 2.0 mL of dichloroethane was added. A phosphine stock solution was prepared from 262 mg of triphenylphosphine and 2.0 mL of solvent. Reaction solutions were prepared by diluting aliquots of the rhodium solution with the phosphine stock solution in order to maintain a constant phosphine concentration. The solutions were placed in nitrogen-flushed reaction tubes, sealed, and heated at 84.7 ± 0.1 °C for 1.0 h. The UV absorbance was obtained, and the concentration was determined from the working graph. A plot of initial rate vs. $[\mathbf{8a}]_0$ gave a slope of 1.

B. $RhCl_2(styryl)(CO)(PPh_3)_2$ (39.8 mg, 0.04 mmol) and 10.8 mg (0.04 mmol) of triphenylphosphine were placed in a flask with side arm. After a nitrogen-vacuum cycle, 4.0 mL of dichloroethane was added. Portions of this solution, 0.4 mL, were added to nitrogen-flushed flasks containing the following amounts of allyltriphenylphosphonium chloride: 27 mg (0.08 mmol), 20.3 mg (0.06 mmol), 13.5 mg (0.04 mmol), 6.7 mg (0.02 mmol), and no salt. After being degassed, the solutions were placed in the reaction tubes and heated for 1.0 h, as described in the previous experiment. A plot of initial rate vs. $[RP^+Ph_3Cl^-]_0$ gave a steep initial slope and a slope of −1 in the region $[RP^+Ph_3Cl^-]_0$ = 0.05–0.2 M.

C. The styryl complex (39.8 mg, 0.04 mmol) and 270 mg (0.8 mmol) of allyltriphenylphosphonium chloride were added to a flask, which had been evacuated and flushed with nitrogen. Dichloroethane, 4.0 mL, was admitted. A 0.4 M phosphine solution was prepared from 104.8 mg (0.4 mmol) of triphenylphosphine and 1 mL of solvent. Aliquots of the stock rhodium complex solution, 0.2 mL, were mixed with varying amounts of the phosphine solution to give the following phosphine concentrations: 0.01 M, 0.02 M, 0.04 M, and 0.05 M. These new solutions are degassed and reacted for 1 h at 84.7 ± 0.1 °C in the usual manner. The amount of reaction is determined by UV spectroscopy with use of the working graph. A plot of the initial rates vs. $[PPh_3]_0$ gave a slope of 1 in the region $[PPh_3]_0$ = 0.01–0.04 M.

Acknowledgment. We are grateful to Johnson-Matthey, Inc., for a generous loan of $RhCl_3$ and to the National Science Foundation (Grant No. NSF-7308798) for financial support. S.H.H. was the recipient of Sherman Clarke and Elon H. Hooker Fellowships from the University of Rochester. We appreciate stimulating discussions with R. H. Grubbs and C. P. Casey and thank D. K. Wedegaertner for the ^{31}P NMR experiments.

A Closed Three-Center Carbon–Hydrogen–Metal Interaction. A Neutron Diffraction Study of $HFe_4(\eta^2\text{-}CH)(CO)_{12}$

M. A. Beno,[1a] Jack M. Williams,*[1a] M. Tachikawa,[1b] and E. L. Muetterties*[1b]

Contribution from the Chemistry Division, Argonne National Laboratory, Argonne, Illinois 60439, Chemistry Department, Brookhaven National Laboratory, Upton, Long Island 11973, and the Department of Chemistry, University of California, Berkeley, California 94720. *Received July 2, 1980*

Abstract: The crystal and molecular structure of $HFe_4(\eta^2\text{-}CH)(CO)_{12}$ has been determined at 173 K by X-ray diffraction and at 26 K by neutron diffraction techniques. The complex crystallized in the monoclinic space group $P2_1/c$ [C_{2h}^5, No. 14] with unit-cell dimensions of a = 8.694 (1) Å, b = 32.920 (6) Å, c = 13.757 (3) Å, β = 112.95 (1)°, and V = 3625.7 Å^3 at 26 K with Z = 8. Full-matrix least-squares refinement of the neutron data gave $R(F_o)$ = 0.060 and $R_w(F_o^2)$ = 0.079 for all 5663 data. The "goodness-of-fit", with a data to parameter ratio of 10.1:1, was 1.876. The only significant structural differences in the two unique molecules of the asymmetric unit were the intermolecular contacts. The iron atoms were arranged in a "butterfly" conformation with a C–H group nestled between the wings. The most significant structural finding was a true C—H—Fe three-center interaction, containing both a very short Fe–H distance of 1.753 (4) Å (1.747 (4) Å, second molecule) and the longest reported C–H bond distance, 1.191 (4) Å (1.176 (4) Å). These results have been discussed in relation to the origin and nature of this C—H—Fe three-center interaction, the "activation" of C–H bonds in catalysis, and possible η^2 bonding of a C–H fragment at a metal surface.

Introduction

In some hydrogenation reactions of carbon monoxide, the sequence comprises dissociative CO chemisorption to give a surface carbide atom that is subsequently hydrogenated.[2] A question of substance in our research which compares the coordination chemistry of metal clusters and metal surfaces has been whether a cluster carbide atom might exhibit reactivity toward hydrogen. Recently, the transformation of $Fe_4C(CO)_{12}^{2-}$ to $Fe_4C(CO)_{12}$ followed by hydrogen addition to give $HFe_4(\eta^2\text{-}CH)(CO)_{12}$ has incisively demonstrated the reactivity of exposed, low coordinate cluster carbide carbon atoms.[3] We describe here the full molecular structure of the end product of these key transformations, $HFe_4(\eta^2\text{-}CH)(CO)_{12}$, and discuss the stereochemical significance

(1) (a) Argonne National Laboratory. (b) University of California.
(2) See discussion by E. L. Muetterties and J. Stein, *Chem. Rev.*, **79**, 479 (1979), and references therein.
(3) M. Tachikawa and E. L. Muetterties, *J. Am. Chem. Soc.*, **102**, 4541 (1980).

0002-7863/81/1503-1485$01.25/0

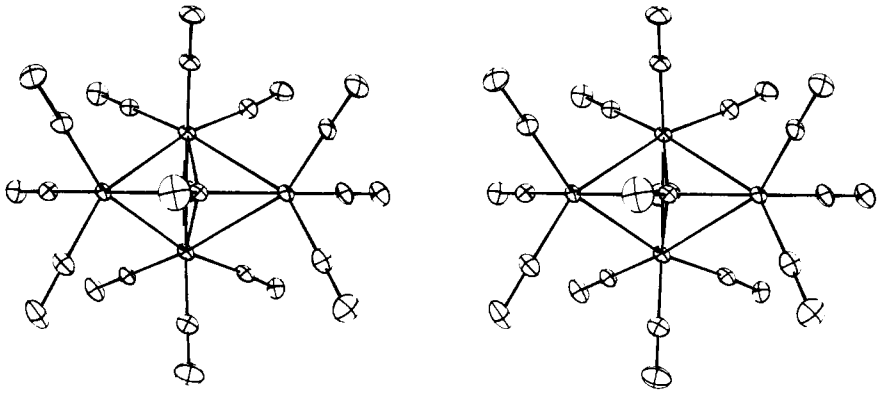

Figure 1. Stereographic ORTEP of the $HFe_4(\eta^2\text{-}CH)(CO)_{12}$ cluster which clearly shows the noncrystallographic mirror plane containing the two apical iron atoms, the C–H ligand, and the bridging hydride atom. Also, this view illustrates the near C_{2v} symmetry of the atoms representative of the $Fe_4(CO)_{12}$ subunit. The hydride atom bridging Fe(2) and Fe(3) is obscured below the methylidyne ligand (see side view in Figure 2.) The thermal ellipsoids in all the figures are scaled to enclose the 75% probability level.

Table I. Experimental Parameters for the 26 K Neutron Diffraction Study of $HFe_4(\eta^2\text{-}CH)(CO)_{12}$

A. Crystal Parameters	
space group $P2_1/c$ [C_{2h}^5, No. 14]	$Z = 8$ molecules/unit cell
cell constants:	$\lambda = 1.1517$ (1) Å (Ge 220, 34° takeoff angle)
$a = 8.694$ (1) Å	$M_r = 573.542$
$b = 32.920$ (6) Å	$\rho_c = 2.101$ g/cm^3
$c = 13.757$ (3) Å	$\mu_c = 0.1944$ cm^{-1}
$\beta = 112.95$ (1) Å	$T_{min} = 0.93$, $T_{max} = 0.97$
$V_{cell} = 3626$ (1) Å^3	
B. Measurement of Intensity Data	
total reflections	6026
total unique reflections	5942
reflections used in least-squares (see text)	5663
reflections with $F^2 > \sigma(F^2)$	5128
$(\sin\theta)/\lambda_{max}$	0.609 Å^{-1}
data to parameter ratio	10.1 (all data), 9.2 ($F_o^2 > \sigma(F_o^2)$)
function minimized in the least-squares refinement	$\Sigma w\lvert F_o^2 - S^2F_c^2\rvert^2$
C. Agreement Factors[a]	
all data	
$R(F_o)$	0.0602
$R(F_o^2)$	0.0656
$R_w(F_o^2)$	0.0790
"goodness-of-fit"	1.876
data where $F_o^2 > \sigma(F_o^2)$	
$R(F_o)$	0.0508
$R(F_o^2)$	0.0631
$R_w(F_o^2)$	0.0772
"goodness-of-fit"	1.937

[a] $R(F_o) = \Sigma\lvert\lvert F_o\rvert - \lvert F_c\rvert\rvert/\Sigma\lvert F_o\rvert$. $R(F_o^2) = \Sigma\lvert F_o^2 - F_c^2\rvert/\Sigma F_o^2$. $R_w(F_o^2) = [\Sigma w\lvert F_o^2 - F_c^2\rvert^2/\Sigma wF_o^4]^{1/2}$. "Goodness-of-fit" = $[\Sigma w(F_o^2 - F_c^2)^2/n - p]^{1/2}$.

of the methylidyne ligand in this cluster molecule. Preliminary reports of this chemistry have been presented.[3,4a] The complex discussed here contains the longest C–H distance in a C–H···metal bond yet reported, and a discussion of this type of three-center interaction important in C–H bond activation has been presented.[4]

Experimental Section

A large (1.6 mm × 3.0 mm × 4.3 mm) well-formed crystal of $HFe_4(\eta^2\text{-}CH)(CO)_{12}$[3] was grown from hexane solution. The crystal was sealed under N_2 in a lead-glass capillary and placed in a helium-filled chamber of a modified closed-cycle helium refrigerator (Air Products and Chemicals, Inc., DISPLEX Model CS-202). Neutron data measurements were made at 26 K on a four-circle diffractometer at the Brookhaven high flux beam reactor.[5] The unit-cell constants were obtained from a least-squares fit of the sin θ values of 29 reflections with 32° ≤ 2θ ≤ 77° (λ = 1.1517 (1) Å). Three-dimensional diffraction data were collected to a maximum $(\sin\theta)/\lambda$ value of 0.609 Å^{-1} by using the θ–2θ step scan technique.

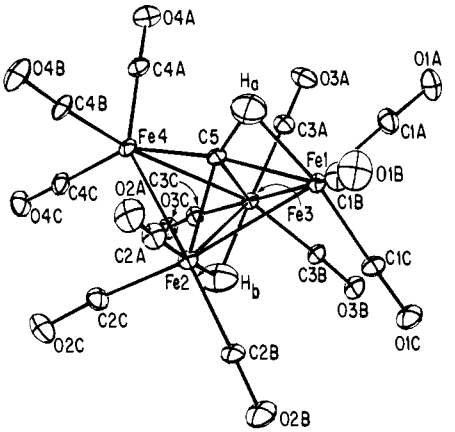

Figure 2. This side view of $HFe_4(\eta^2\text{-}CH)(CO)_{12}$ shows the atom-labeling scheme.

Profiles for 279 reflections showed considerable overlap of the diffraction peaks due to the lack of instrumental resolution concerning the long (~33 Å) b axis, and these intensities were omitted from the least-squares refinement. The intensities of two check reflections monitored periodically throughout data collection were invariant with time. A total of 5663 independent diffraction intensities were observed (excluding those reflections omitted for peak overlap); of these 5128 possessed $I_0 < \sigma I_0$. The data were corrected for Lorentz effects, and an analytical absorption correction[6] was applied. A summary of the experimental parameters is given in Table I.

The structural parameters were refined by using the coordinates previously reported[4a] for the −100 °C X-ray structure, and isotropic temperature factors were initially set at B = 1.0 Å^2. In the final cycles of the full-matrix least-squares refinement, all atom parameters were included with anisotropic temperature factors and a secondary extinction parameter[7] (g = 0.34 (1) × 10^{-4}) was refined. The final agreement factors for all 5663 independent data were $R(F_o^2)$ = 0.066, $R_w(F_o^2)$ = 0.079, and "goodness-of-fit" = 1.876. A difference Fourier map calculated from the final coordinates was virtually featureless.

Final positional and thermal parameters are given in Table II. A listing of the observed and calculated structure factors is given as supplementary material to this paper. The neutron scattering amplitudes

(4) (a) M. A. Beno, J. M. Williams, M. Tachikawa, and E. L. Muetterties, *J. Am. Chem. Soc.*, **102**, 4542 (1980); (b) R. K. Brown, J. M. Williams, A. J. Schultz, G. D. Stucky, S. D. Ittel, and R. L. Harlow, *ibid.*, **102**, 981 (1980), and references therein.

(5) (a) R. K. McMullen, L. C. Andrews, T. F. Koetzle, F. Reidinger, R. Thomas, and G. J. B. Williams, Neutron and X-ray Data Acquisition System (NEXDAS), unpublished work, 1976. (b) D. G. Dimmler, N. Greenlaw, M. A. Kelley, D. W. Potter, S. Rankowitz, and F. W. Stubblefield, *IEEE Trans Nucl. Sci.*, **NS-23**, 398 (1976).

(6) J. DeMuelenaer and H. Tompa, *Acta Crystallogr.*, **19**, 1014 (1965).

(7) W. A. Zachariasen, *Acta Crystallogr., Sect. A*, **24**, 421 (1968); P. Coppens and W. C. Hamilton, *ibid.*, **26**, 71 (1970).

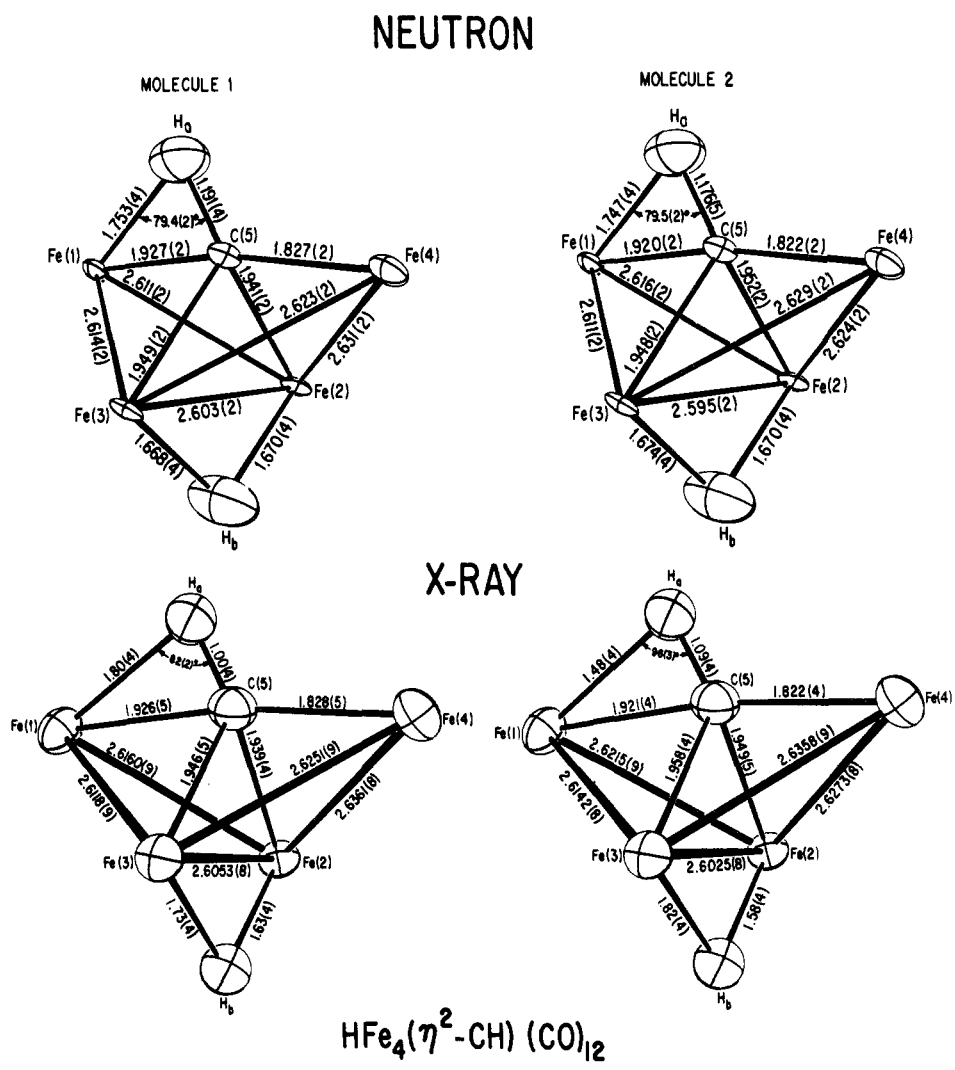

Figure 3. Cluster skeleton distances from 26 K neutron and 173 K X-ray[4a] diffraction investigations. The three-center CHFe interaction, **1**, contains both a carbon–metal bond of length 1927 (2) Å (1.920 (1) Å) and a hydrogen–iron distance of 1.753 (4) Å (1.747 (4) Å). The C(5)–H_a bond distance of 1.191 (4) Å is the longest yet observed in a crystalline compound. The differences in the hydrogen positional parameters observed in the neutron and X-ray cases highlight the great utility of neutron diffraction in high precision low-temperature crystallographic investigations.

used were $b_{Fe} = 0.95$, $b_O = 0.58$, $b_C = 0.665$, and $b_H = -0.374$ (all in units of 10^{-12} cm).

Results and Discussion

The Basic Structure. The molecular structure of $HFe_4(\eta^2\text{-}CH)(CO)_{12}$, as established by X-ray[4a] and neutron diffraction studies, has a butterfly array of four iron atoms with an η^2 methylidyne ligand in which the carbon atom is bonded to all four iron atoms and the CH hydrogen atom forms a strong, closed[8a] three-center, **1**, bond (Figures 1 and 2). The hydride hydrogen

1

atom, H_b, bridges the basal iron–iron bond. Each iron atom is terminally bonded to three carbonyl groups. The bond distances and angles for $HFe_4(\eta^2\text{-}CH)(CO)_{12}$ are given in Tables III and IV, respectively. An examination of these tables and the stereoview of the cluster displayed in Figure 1 establishes two key points. One is that the deviations in the bond distances and angles between the two crystallographically independent molecules are small[8b] (the maximal differences in analogous bond distances and angles are 0.015 Å and 5°, about 6σ). The second is that the molecule possesses an almost perfect noncrystallographic mirror plane containing the two apical iron atoms Fe(1) and Fe(4), the η^2-methylidyne ligand (C(5)–H_a), and the bridging hydride, H_b. In fact, Figure 1 clearly shows the approximate C_{2v} symmetry of the cluster, discounting only the presence of the C–H group. The numbering scheme used for both independent molecules of the asymmetric unit is given in Figure 2.

A drawing of the iron cluster that clearly illustrates the C–H–metal interaction is presented in Figure 3 for both the 26 K neutron diffraction data and the previously reported[4] 173 K X-ray diffraction study. The unique ability of neutron diffraction to provide structural parameters of comparable accuracy for all atoms regardless of atomic number is clearly illustrated. The standard deviations of the bond distances are in the range of 0.002–0.005 Å in the neutron case while those for the X-ray results vary from 0.0008 to 0.04 Å. Comparison of chemically equivalent bond distances (e.g., Fe(2)–H_b and Fe(3)–H_b) shows that in the X-ray case the errors in the hydrogen positions are much larger than the esd's, on the order of 0.1–0.2 Å.

(8) (a) Cf. discussions in "Boron Hydride Chemistry", E. L. Muetterties, Ed., Academic Press New York, 197 Chapters 1-3. (b) In a case such as this in which $z = 8$, rather than 4, where two independent molecules comprise the asymmetric unit, one must be certain that symmetry elements have not been overlooked. However, the X-ray derived cell parameters (from films and diffractometer data) were independently verified with the use of randomly collected neutron diffraction data and autoindexing (program BLIND)[8c] which gave the same unit cell parameters as derived for the X-ray case. In addition, the full-matrix least-squares refinement of the neutron and X-ray data proceeded smoothly and led to chemically reasonable structural parameters. Decisive proof of the independence of the two molecules is found in the intermolecular contacts given in Table V, which show that the molecules are situated in slightly different chemical environments. (c) R. A. Jacobson, *J. Appl. Crystallogr.*, **9**, 115 (1976).

Table II. Positional[a] and Thermal[b] Parameters (Å²) for $HFe_4(\eta^2\text{-}CH)(CO)_{12}$

atom	x	y	z	U_{11}	U_{22}	U_{33}	U_{12}	U_{13}	U_{23}
Fe(1)	0.8583 (2)	0.251 00 (4)	0.7645 (1)	0.009 (1)	0.006 (1)	0.003 (1)	−0.001 (1)	0.001 (1)	−0.0002 (5)
Fe(2)	0.8916 (2)	0.172 27 (4)	0.7605 (1)	0.008 (1)	0.007 (1)	0.002 (1)	−0.000 (1)	0.000 (1)	−0.0011 (5)
Fe(3)	0.6036 (2)	0.205 68 (4)	0.6531 (1)	0.009 (1)	0.007 (1)	0.002 (1)	−0.000 (1)	0.001 (1)	−0.0001 (5)
Fe(4)	0.6404 (2)	0.161 18 (4)	0.8189 (1)	0.008 (1)	0.008 (1)	0.003 (1)	−0.000 (1)	0.001 (1)	0.0004 (5)
C(5)	0.7477 (2)	0.206 83 (6)	0.8028 (1)	0.010 (1)	0.008 (1)	0.004 (1)	0.000 (1)	0.003 (1)	−0.000 (1)
C(1A)	0.7493 (3)	0.298 79 (6)	0.7459 (1)	0.016 (1)	0.009 (1)	0.010 (1)	0.001 (1)	0.004 (1)	0.001 (1)
O(1A)	0.6776 (3)	0.328 88 (7)	0.7316 (2)	0.023 (1)	0.009 (1)	0.021 (1)	0.002 (1)	0.010 (1)	0.005 (1)
C(1B)	1.0590 (3)	0.266 04 (6)	0.8635 (1)	0.013 (1)	0.012 (1)	0.006 (1)	−0.002 (1)	0.000 (1)	−0.001 (1)
O(1B)	1.1839 (3)	0.275 98 (8)	0.9253 (2)	0.013 (1)	0.018 (1)	0.010 (1)	−0.005 (1)	−0.001 (1)	−0.002 (1)
C(1C)	0.9208 (2)	0.258 79 (6)	0.6560 (1)	0.011 (1)	0.011 (1)	0.006 (1)	−0.000 (1)	0.003 (1)	−0.001 (1)
O(1C)	0.9593 (3)	0.264 42 (7)	0.5872 (2)	0.016 (1)	0.016 (1)	0.008 (1)	−0.001 (1)	0.006 (1)	0.000 (1)
C(2A)	1.0539 (2)	0.173 88 (6)	0.8915 (1)	0.011 (1)	0.010 (1)	0.004 (1)	0.000 (1)	−0.001 (1)	−0.000 (1)
O(2A)	1.1520 (3)	0.174 19 (7)	0.9753 (2)	0.012 (1)	0.015 (1)	0.005 (1)	0.001 (1)	−0.001 (1)	0.001 (1)
C(2B)	1.0276 (2)	0.175 26 (6)	0.6882 (1)	0.010 (1)	0.011 (1)	0.005 (1)	0.001 (1)	0.003 (1)	−0.002 (1)
O(2B)	1.1090 (3)	0.176 26 (8)	0.6405 (2)	0.019 (1)	0.018 (1)	0.008 (1)	−0.001 (1)	0.007 (1)	−0.002 (1)
C(2C)	0.8707 (3)	0.117 80 (6)	0.7540 (1)	0.013 (1)	0.008 (1)	0.009 (1)	−0.000 (1)	0.004 (1)	−0.002 (1)
O(2C)	0.8686 (3)	0.082 90 (7)	0.7485 (2)	0.017 (1)	0.009 (1)	0.015 (1)	0.002 (1)	0.004 (1)	−0.001 (1)
C(3A)	0.4535 (3)	0.240 89 (6)	0.6651 (1)	0.011 (1)	0.011 (1)	0.007 (1)	0.001 (1)	0.002 (1)	−0.001 (1)
O(3A)	0.3594 (3)	0.263 07 (8)	0.6742 (2)	0.017 (1)	0.014 (1)	0.014 (1)	0.005 (1)	0.005 (1)	−0.002 (1)
C(3B)	0.5996 (3)	0.225 47 (6)	0.5294 (1)	0.012 (1)	0.010 (1)	0.005 (1)	0.001 (1)	0.003 (1)	0.002 (1)
O(3B)	0.5962 (3)	0.236 47 (7)	0.4503 (2)	0.023 (1)	0.013 (1)	0.006 (1)	0.001 (1)	0.006 (1)	0.003 (1)
C(3C)	0.4558 (2)	0.165 52 (6)	0.5944 (1)	0.012 (1)	0.009 (1)	0.005 (1)	0.000 (1)	0.001 (1)	0.000 (1)
O(3C)	0.3608 (3)	0.141 37 (7)	0.5481 (2)	0.012 (1)	0.011 (1)	0.008 (1)	−0.004 (1)	0.002 (1)	−0.003 (1)
C(4A)	0.4695 (3)	0.181 53 (6)	0.8433 (1)	0.016 (1)	0.011 (1)	0.006 (1)	−0.000 (1)	0.005 (1)	−0.000 (1)
O(4A)	0.3633 (3)	0.195 96 (8)	0.8614 (2)	0.015 (1)	0.017 (1)	0.013 (1)	−0.001 (1)	0.007 (1)	−0.002 (1)
C(4B)	0.7515 (2)	0.148 02 (6)	0.9544 (1)	0.011 (1)	0.012 (1)	0.004 (1)	−0.002 (1)	0.002 (1)	0.002 (1)
O(4B)	0.8185 (3)	0.141 24 (8)	1.0424 (2)	0.015 (1)	0.019 (1)	0.005 (1)	−0.002 (1)	0.000 (1)	0.004 (1)
C(4C)	0.5501 (3)	0.110 87 (6)	0.7734 (1)	0.016 (1)	0.009 (1)	0.006 (1)	−0.001 (1)	0.003 (1)	0.001 (1)
O(4C)	0.4920 (3)	0.079 21 (7)	0.7464 (2)	0.019 (1)	0.007 (1)	0.012 (1)	−0.003 (1)	0.004 (1)	−0.002 (1)
H_a	0.7842 (6)	0.235 4 (1)	0.8603 (3)	0.031 (2)	0.020 (2)	0.015 (2)	−0.003 (2)	0.008 (2)	−0.006 (2)
H_b	0.7422 (5)	0.173 6 (1)	0.6390 (3)	0.020 (2)	0.033 (3)	0.014 (2)	0.004 (2)	0.004 (2)	−0.004 (2)
Fe(1)P	0.2775 (2)	0.027 20 (4)	0.1650 (1)	0.008 (1)	0.005 (1)	0.002 (1)	−0.000 (1)	0.000 (1)	−0.0002 (5)
Fe(2)P	0.4084 (2)	0.087 13 (4)	0.2963 (1)	0.010 (1)	0.006 (1)	0.001 (1)	0.001 (1)	0.0019 (5)	0.0000 (5)
Fe(3)P	0.5597 (2)	0.059 79 (4)	0.1802 (1)	0.009 (1)	0.006 (1)	0.001 (1)	0.000 (1)	0.001 (1)	0.0000 (5)
Fe(4)P	0.6889 (2)	0.046 73 (4)	0.3848 (1)	0.008 (1)	0.008 (1)	0.002 (1)	−0.001 (1)	0.0008 (5)	0.0002 (5)
C5P	0.4886 (2)	0.032 97 (6)	0.2819 (1)	0.008 (1)	0.010 (1)	0.001 (1)	−0.001 (1)	0.001 (1)	0.000 (1)
C(1A)P	0.2567 (3)	−0.015 95 (6)	0.0790 (1)	0.014 (1)	0.010 (1)	0.004 (1)	−0.001 (1)	0.001 (1)	−0.001 (1)
O(1A)P	0.2418 (3)	−0.043 32 (7)	0.0256 (2)	0.017 (1)	0.013 (1)	0.008 (1)	0.000 (1)	0.005 (1)	−0.005 (1)
C(1B)P	0.1043 (3)	0.014 41 (6)	0.2015 (1)	0.011 (1)	0.010 (1)	0.005 (1)	−0.000 (1)	0.002 (1)	0.000 (1)
O(1B)P	−0.0037 (3)	0.006 08 (7)	0.2246 (2)	0.013 (1)	0.015 (1)	0.012 (1)	−0.000 (1)	0.008 (1)	0.001 (1)
C(1C)P	0.1645 (3)	0.062 16 (6)	0.0628 (1)	0.011 (1)	0.011 (1)	0.004 (1)	0.001 (1)	0.001 (1)	0.003 (1)
O(1C)P	0.0897 (3)	0.083 80 (7)	−0.0042 (2)	0.016 (1)	0.012 (1)	0.009 (1)	0.002 (1)	0.000 (1)	0.004 (1)
C(2A)P	0.3045 (3)	0.070 43 (6)	0.3796 (1)	0.012 (1)	0.010 (1)	0.005 (1)	−0.001 (1)	0.004 (1)	0.001 (1)
O(2A)P	0.2393 (3)	0.059 28 (7)	0.4319 (2)	0.020 (1)	0.013 (1)	0.007 (1)	−0.001 (1)	0.007 (1)	−0.000 (1)
C(2B)P	0.2542 (2)	0.126 27 (6)	0.2312 (1)	0.011 (1)	0.009 (1)	0.005 (1)	−0.001 (1)	0.001 (1)	0.001 (1)
O(2B)P	0.1635 (3)	0.152 42 (7)	0.1955 (2)	0.015 (1)	0.012 (1)	0.011 (1)	0.005 (1)	0.001 (1)	0.004 (1)
C(2C)P	0.5517 (2)	0.121 55 (6)	0.3876 (1)	0.011 (1)	0.011 (1)	0.004 (1)	−0.000 (1)	0.003 (1)	−0.001 (1)
O(2C)P	0.6325 (3)	0.146 79 (7)	0.4411 (2)	0.012 (1)	0.011 (1)	0.008 (1)	−0.001 (1)	0.002 (1)	−0.006 (1)
C(3A)P	0.6115 (2)	0.012 53 (6)	0.1357 (1)	0.012 (1)	0.009 (1)	0.004 (1)	0.001 (1)	0.002 (1)	−0.001 (1)
O(3A)P	0.6427 (3)	−0.018 15 (7)	0.1088 (2)	0.014 (1)	0.010 (1)	0.009 (1)	0.001 (1)	0.003 (1)	−0.003 (1)
C(3B)P	0.4810 (2)	0.085 61 (6)	0.0536 (1)	0.012 (1)	0.009 (1)	0.003 (1)	0.001 (1)	0.002 (1)	0.001 (1)
O(3B)P	0.4346 (3)	0.103 56 (7)	−0.0233 (2)	0.019 (1)	0.012 (1)	0.005 (1)	−0.000 (1)	0.003 (1)	0.004 (1)
C(3C)P	0.7679 (2)	0.080 84 (6)	0.2226 (1)	0.010 (1)	0.009 (1)	0.005 (1)	0.000 (1)	0.001 (1)	−0.001 (1)
O(3C)P	0.8977 (3)	0.094 02 (7)	0.2400 (2)	0.009 (1)	0.013 (1)	0.009 (1)	−0.002 (1)	0.002 (1)	0.000 (1)
C(4A)P	0.8079 (2)	0.002 06 (6)	0.3871 (1)	0.012 (1)	0.010 (1)	0.005 (1)	0.002 (1)	0.001 (1)	0.001 (1)
O(4A)P	0.8791 (3)	−0.027 14 (7)	0.3878 (2)	0.019 (1)	0.012 (1)	0.010 (1)	0.006 (1)	0.004 (1)	0.000 (1)
C(4B)P	0.6626 (2)	0.035 63 (6)	0.5041 (1)	0.012 (1)	0.011 (1)	0.005 (1)	−0.001 (1)	0.003 (1)	0.001 (1)
O(4B)P	0.6402 (3)	0.028 68 (7)	0.5794 (2)	0.015 (1)	0.015 (1)	0.005 (1)	−0.001 (1)	0.005 (1)	0.001 (1)
C(4C)P	0.8656 (2)	0.082 14 (6)	0.4457 (1)	0.009 (1)	0.013 (1)	0.006 (1)	−0.002 (1)	0.001 (1)	−0.001 (1)
O(4C)P	0.9725 (3)	0.104 46 (7)	0.4846 (2)	0.011 (1)	0.012 (1)	0.011 (1)	−0.003 (1)	0.001 (1)	−0.002 (1)
H_aP	0.4203 (5)	0.001 6 (1)	0.2741 (3)	0.030 (2)	0.017 (2)	0.018 (2)	0.002 (2)	0.006 (2)	0.001 (2)
H_bP	0.4936 (6)	0.103 3 (1)	0.2135 (3)	0.033 (3)	0.018 (2)	0.024 (2)	0.000 (2)	0.019 (2)	0.001 (2)

[a] x, y, and z are fractional coordinates. Estimated standard deviations in parentheses. [b] Form of the anisotropic temperature factor is $\exp[-2\pi^2(U_{11}h^2a^{*2} + \ldots + 2U_{12}hka^*b^* + \ldots)]$.

Although the intramolecular distances and angles for both independent molecules are very similar, the intermolecular contacts for the two molecules given in Table V differ greatly. Both molecules appear to be involved in a hydrogen bond formed between the hydrogen of the CH ligand and a carbonyl group bonded to a basal iron atom. Hydrogen atom, H_a, of molecule 1 is 2.574 (4) Å from O(3B) of molecule 1 (produced by a glide plane symmetry operation), while H_a of molecule 2 is 2.485 (5) Å distant from O(4B) of molecule 2 (produced by a center of symmetry). The chains of independent molecules produced by these hydrogen bonds are connected by a more distant O(1A)–H_b (of molecule 2) interaction at 2.697 (5) Å. The participation of the hydrogen atom of the methylidyne ligand in these normal hydrogen bonds with carbonyl oxygens is indicative of its acidic nature as previously shown in chemical studies.[3]

Cluster Framework Structure. Iron–iron distances in the butterfly framework of this cluster fall in the narrow range of 2.595–2.631 Å (both molecules) and average 2.619 (9) Å. This appears to be a normal iron–iron value for iron cluster molecules or molecular ions;[9] in fact, the average Fe–Fe distance should be

Table III. Bond Distances (Å) for $HFe_4(\eta^2\text{-CH})(CO)_{12}$ at 26 K[a]

	molecule 1	molecule 2
	Fe-Fe Distances	
Fe(1)-Fe(2)	2.611 (2)	2.616 (2)
Fe(1)-Fe(3)	2.614 (2)	2.611 (2)
Fe(2)-Fe(3)	2.603 (2)	2.595 (2)
Fe(2)-Fe(4)	2.631 (2)	2.624 (2)
Fe(3)-Fe(4)	2.623 (2)	2.629 (2)
	Fe-CH Distances	
Fe(1)-C(5)	1.927 (2)	1.920 (2)
Fe(1)-H_a	1.753 (4)	1.747 (4)
Fe(2)-C(5)	1.941 (2)	1.952 (2)
Fe(3)-C(5)	1.949 (2)	1.948 (2)
Fe(4)-C(5)	1.827 (2)	1.822 (2)
	H Distances	
H_a-C(5)	1.191 (4)	1.176 (5)
H_b-Fe(2)	1.670 (4)	1.670 (4)
H_b-Fe(3)	1.668 (4)	1.674 (4)
	Fe-CO Distances	
Fe(1)-C(1A)	1.802 (2)	1.812 (2)
Fe(1)-C(1B)	1.814 (2)	1.813 (2)
Fe(1)-C(1C)	1.795 (2)	1.786 (2)
Fe(2)-C(2A)	1.805 (2)	1.800 (2)
Fe(2)-C(2B)	1.820 (2)	1.823 (2)
Fe(2)-C(2C)	1.801 (2)	1.788 (2)
Fe(3)-C(3A)	1.800 (2)	1.792 (2)
Fe(3)-C(3B)	1.810 (2)	1.815 (2)
Fe(3)-C(3C)	1.801 (2)	1.809 (2)
Fe(4)-C(4A)	1.777 (2)	1.792 (2)
Fe(4)-C(4B)	1.786 (2)	1.780 (2)
Fe(4)-C(4C)	1.835 (2)	1.848 (2)
	C-O Distances	
C(1A)-O(1A)	1.146 (3)	1.138 (3)
C(1B)-O(1B)	1.135 (3)	1.135 (3)
C(1C)-O(1C)	1.136 (3)	1.146 (3)
C(2A)-O(2A)	1.136 (3)	1.136 (3)
C(2B)-O(2B)	1.137 (3)	1.141 (3)
C(2C)-O(2C)	1.151 (3)	1.150 (3)
C(3A)-O(3A)	1.140 (3)	1.144 (3)
C(3B)-O(3B)	1.138 (3)	1.140 (3)
C(3C)-O(3C)	1.145 (3)	1.144 (3)
C(4A)-O(4A)	1.149 (3)	1.141 (3)
C(4B)-O(4B)	1.142 (3)	1.149 (3)
C(4C)-O(4C)	1.155 (3)	1.141 (3)

[a] Estimated standard deviations are given in parentheses.

within ~0.06 Å of this average value of 2.62 Å provided that the cluster is coordinately saturated. Directly relevant in this specific comparison, and for other discussions of the structural features of $HFe_4(\eta^2\text{-CH})(CO)_{12}$, are a set of iron butterfly clusters: $[HFe_4(\eta^2\text{-CO})(CO)_{12}^-]$[13] (**2**), $[HFe_4C(CO)_{12}^-]$[14] (**3**), $Fe_4C(CO)_{13}$[15] (**4**), and $[Fe_4(CCOOCH_3)(CO)_{12}^-]$[16] (**5**) (Chart I). Explicitly isostructural and isoelectronic to $HFe_4(\eta^2\text{-CH})(CO)_{12}$ is **2**, and here the average Fe-Fe separation is 2.627 (5) Å.[13] Derivatives of $HFe_4(\eta^2\text{-CH})(CO)_{12}$ are the carbides $[HFe_4C(CO)_{12}^-]$ and $Fe_4C(CO)_{13}$ where the average Fe-Fe distances are 2.621 (9) and 2.622 (1) Å, respectively.[14,15] All these butterfly structures are 62-electron[17] structures. Formally electron deficient is $[Fe_4(CCOOCH_3)(CO)_{12}^-]$, and the Fe-Fe distances in this nominally unsaturated species are significantly smaller with a range of 2.496 (1)–2.590 (1) Å (average 2.521 Å).[5-18]

A shape parameter for butterfly clusters that appears to be more sensitive to subtle electronic features in a cluster than are the metal–metal distances is the wing set, i.e., the dihedral angle, δ_w, between the planes defined by the two basal iron atoms with each of the apical iron atoms (Fe(1) and Fe(4) as noted in Figure 2). These values[19] are listed in Table VI; obviously related to δ_w are the Fe_{apical}–C–Fe_{apical} angles and Fe–C distances, and these are included in Table VI. For the 62-electron clusters, δ_w (average) is 108 (7)° and the primary factor that contributes to the shape parameter for these clusters is the iron–carbon distance. The δ_w value for the one 60-electron cluster, **5**, is substantially larger, 130°, and this is largely a reflection of two unique features in this cluster, the short Fe–Fe bonds, and the "bent" Fe_{apical}–C–Fe_{apical} connection.

The η^2-CH and μ-H Ligands. Characterization of the η^2-methylidyne ligand in this structure as a three-center two-electron bond was fully discussed and compared with relevant structures with C–H–M interactions in the preliminary communications based on the X-ray study and the chemistry of this molecule.[3,4a] This C–H–Fe interaction is a tight and closed[8] three-center two-electron bond[4a] and is unique among all known C–H–metal interactions in molecular complexes in having a short carbon–metal separation in addition to long C–H and short H–metal separations.[4b] We only need to add here that with the more precise neutron determined position of the methylidyne hydrogen atom that the C–H distances are very large, 1.191 (4) and 1.176 (4) Å, in molecules 1 and 2. These distances are consistent with the observations (i) that facile extraction of this hydrogen atom as a proton is effected by weak bases like methanol and (ii) that hydrogen atom site exchange between the three-center C–H–Fe site (**1**) and the bridging Fe–H–Fe site occurs at a rate detectable by NMR spin saturation experiments.[3] The neutron-determined values of the H–Fe(1) separations in the three-center bond are 1.753 (4) and 1.747 (4) Å for molecules 1 and 2, values that are only slightly larger than the average value of 1.67 Å for the hydride hydrogen atom bridging the basal iron atoms in this cluster. The general bonding and chemical significance of this unique η^2-methylidyne ligand vis-à-vis metal surface coordination chemistry was concisely presented earlier.[3,4a] In addition, there are other features of the η^2-CH ligand established from this neutron crystallographic analysis and from chemical and spectroscopic data that merit comment with respect to the surface-cluster analogy. The acidic character of the hydrogen atom in the methylidyne ligand of the cluster should also prevail for the metal surface case if the metal is sufficiently electropositive to bind a CH fragment in an η^2 fashion. Thus strongly basic sites on supported metals could significantly alter the course of a hydrocarbon reaction or of a CO hydrogenation reaction that proceeds through CH surface intermediates. Certainly the facile hydrogen atom site exchange between C(5)-H_b-Fe(1) and Fe(2)-H_a-Fe(3) sites established for the cluster is a formal analogue of the pervasive and rapid H–D exchange of hydrogen atoms between hydrocarbons and deuterium atoms chemisorbed on metal surfaces.

The interaction of the carbon atom of the methylidyne ligand is nearly central above the wings of the Fe_4 butterfly. However, the Fe(4)–C bond distance is substantially shorter than the other three: 1.827 (2) Å compared with values of 1.927 (2), 1.941 (2), and 1.949 (2) Å for iron atoms (1), (2), and (3), respectively (the average difference is ~50σ). A similar pattern of Fe–C distances

(9) The range[10] of iron–iron distances in iron clusters is 2.56–2.71 Å with an average value near 2.64 Å. All these are coordinately saturated clusters. For molecular iron carbide clusters of cage form (carbon within a metal polyhedron[11]) and of peripheral Fe_5C form, the range in iron–iron distances is 2.63–2.69 Å.[11] Binary iron carbides are of two types, one with octahedral Fe_6C units and the other with trigonal prismatic Fe_6C units, and the respective average Fe–Fe distances are 2.72 and 2.63 Å.[11] Body-centered cubic iron metal has an Fe–Fe separation of 2.4823 Å at 20 °C.[12]

(10) E. L. Muetterties, T. N. Rhodin, E. Band, C. F. Brucker, and W. R. Pretzer, *Chem. Rev.*, **79**, 91 (1979).

(11) M. Tachikawa and E. L. Muetterties, *Prog. Inorg. Chem.*, in press.

(12) "Handbook of Chemistry and Physics", 55th ed., CRC Press, Cleveland, Ohio 1974, p F-201.

(13) (a) M. Manassero, M. Sansoni, and G. Longoni, *J. Chem. Soc., Chem. Commun.*, 919 (1976). (b) M. Manassero, private communication.

(14) K. Whitmire, E. Holt, and D. F. Shriver, private communication.

(15) J. S. Bradley, private communication.

(16) J. S. Bradley, G. B. Ansell, and M. E. Hill, *J. Am. Chem. Soc.*, **101**, 7417 (1979).

(17) Qualitative and general molecular orbital considerations indicate that a 62-electron four-metal cluster should generally have a butterfly arrangement, cf. J. W. Lauher, *J. Am. Chem. Soc.*, **100**, 5305 (1978).

(18) No error estimates were originally reported,[16] but cited data were obtained from J. S. Bradley.[15]

(19) In each of these butterfly structures, there is a carbon atom bonded to each of the four iron atoms and with the exception of 3 and 4 to one other atom (H, O, or C).

Table IV. Bond Angles (Deg) for $HFe_4(\eta^2\text{-}CH)(CO)_{12}$ at 26 K[a]

	molecule 1	molecule 2
Angles in the Fe_4 Cluster		
Fe(2)-Fe(1)-Fe(3)	59.76 (5)	59.53 (5)
Fe(2)-Fe(1)-C(5)	47.77 (7)	48.03 (7)
Fe(2)-Fe(1)-H_a	78.6 (1)	78.4 (1)
Fe(3)-Fe(1)-C(5)	47.96 (7)	48.01 (7)
Fe(3)-Fe(1)-H_a	78.4 (1)	78.4 (2)
Fe(1)-Fe(2)-Fe(3)	60.20 (5)	60.14 (5)
Fe(1)-Fe(2)-Fe(4)	91.16 (5)	90.79 (5)
Fe(1)-Fe(2)-H_b	86.8 (2)	87.7 (2)
Fe(1)-Fe(2)-C(5)	47.42 (7)	46.99 (6)
Fe(3)-Fe(2)-Fe(4)	60.16 (5)	60.49 (5)
Fe(3)-Fe(2)-H_b	38.8 (1)	39.2 (1)
Fe(3)-Fe(2)-C(5)	48.13 (7)	48.23 (7)
Fe(4)-Fe(2)-H_b	84.0 (2)	84.2 (2)
C(5)-Fe(2)-H_b	86.8 (2)	87.2 (2)
Fe(1)-Fe(3)-Fe(2)	60.07 (5)	60.33 (5)
Fe(1)-Fe(3)-Fe(4)	91.24 (5)	90.79 (6)
Fe(1)-Fe(3)-H_b	86.8 (2)	87.8 (2)
Fe(1)-Fe(3)-C(5)	47.33 (6)	47.10 (6)
Fe(2)-Fe(3)-Fe(4)	60.45 (5)	60.30 (5)
Fe(2)-Fe(3)-H_b	38.8 (1)	39.1 (1)
Fe(2)-Fe(3)-C(5)	47.87 (7)	48.37 (7)
Fe(4)-Fe(3)-H_b	84.3 (2)	84.0 (1)
C(5)-Fe(3)-H_b	86.6 (2)	87.3 (2)
Fe(2)-Fe(4)-Fe(3)	59.39 (5)	59.21 (5)
Fe(2)-Fe(4)-C(5)	47.52 (7)	48.05 (7)
Fe(3)-Fe(4)-C(5)	47.95 (7)	47.81 (7)
Fe(2)-H_b-Fe(3)	62.0 (1)	61.7 (1)
Angles Involving the CH Group		
Fe(1)-C(5)-Fe(2)	84.75 (8)	84.98 (9)
Fe(1)-C(5)-Fe(3)	84.70 (9)	84.90 (8)
Fe(1)-C(5)-Fe(4)	170.5 (1)	170.8 (1)
Fe(1)-C(5)-H_a	63.9 (2)	63.5 (2)
Fe(2)-C(5)-Fe(3)	84.00 (9)	83.40 (9)
Fe(2)-C(5)-Fe(4)	88.5 (1)	88.0 (1)
Fe(2)-C(5)-H_a	128.8 (3)	128.6 (3)
Fe(3)-C(5)-Fe(4)	87.93 (9)	88.3 (1)
Fe(3)-C(5)-H_a	127.7 (2)	128.6 (2)
Fe(4)-C(5)-H_a	125.9 (2)	125.8 (2)
C(5)-H_a-Fe(1)	79.4 (2)	79.5 (2)
Fe-CO Angles		
Fe(2)-Fe(1)-C(1A)	156.9 (1)	161.4 (1)
Fe(2)-Fe(1)-C(1B)	101.82 (9)	99.72 (8)
Fe(2)-Fe(1)-C(1C)	92.97 (9)	90.87 (8)
Fe(3)-Fe(1)-C(1A)	97.86 (9)	103.03 (9)
Fe(3)-Fe(1)-C(1B)	160.5 (1)	158.39 (9)
Fe(3)-Fe(1)-C(1C)	93.21 (8)	90.54 (9)
C(5)-Fe(1)-C(1A)	114.0 (1)	116.3 (1)
C(5)-Fe(1)-C(1B)	115.9 (1)	114.7 (1)
C(5)-Fe(1)-C(1C)	132.9 (1)	130.4 (1)
H_a-Fe(1)-C(1A)	92.0 (2)	92.3 (2)
H_a-Fe(1)-C(1B)	92.5 (2)	92.2 (2)
H_a-Fe(1)-C(1C)	170.3 (2)	167.4 (2)
C(1A)-Fe(1)-C(1B)	99.6 (1)	96.7 (1)
C(1A)-Fe(1)-C(1C)	94.0 (1)	96.1 (1)
C(1B)-Fe(1)-C(1C)	94.1 (1)	96.1 (1)
Fe(1)-Fe(2)-C(2A)	90.83 (9)	91.04 (8)
Fe(1)-Fe(2)-C(2B)	93.37 (9)	98.95 (8)
Fe(1)-Fe(2)-C(2C)	168.47 (8)	163.7 (1)
Fe-CO Angles		
Fe(3)-Fe(2)-C(2A)	139.87 (9)	141.92 (9)
Fe(3)-Fe(2)-C(2B)	110.69 (9)	113.28 (8)
Fe(3)-Fe(2)-C(2C)	109.66 (9)	105.71 (9)
Fe(4)-Fe(2)-C(2A)	96.63 (9)	98.96 (8)
Fe(4)-Fe(2)-C(2B)	165.48 (9)	163.5 (1)
Fe(4)-Fe(2)-C(2C)	78.28 (9)	74.20 (8)
C(5)-Fe(2)-C(2A)	92.0 (1)	94.2 (1)
C(5)-Fe(2)-C(2B)	139.9 (1)	145.0 (1)
C(5)-Fe(2)-C(2C)	122.3 (1)	118.1 (1)
H_b-Fe(2)-C(2A)	177.6 (2)	176.6 (2)
H_b-Fe(2)-C(2B)	82.5 (2)	82.9 (2)
H_b-Fe(2)-C(2C)	87.3 (2)	84.5 (2)
C(2A)-Fe(2)-C(2B)	97.1 (1)	94.2 (1)
C(2A)-Fe(2)-C(2C)	95.1 (1)	97.5 (1)
C(2B)-Fe(2)-C(2C)	95.8 (1)	94.3 (1)
Fe(1)-Fe(3)-C(3A)	93.29 (8)	88.23 (9)
Fe(1)-Fe(3)-C(3B)	92.65 (8)	97.17 (9)
Fe(1)-Fe(3)-C(3C)	165.35 (9)	166.88 (9)
Fe(2)-Fe(3)-C(3A)	142.31 (9)	140.01 (9)
Fe(2)-Fe(3)-C(3B)	111.32 (9)	109.64 (9)
Fe(2)-Fe(3)-C(3C)	107.75 (9)	110.60 (8)
Fe(4)-Fe(3)-C(3A)	97.29 (9)	99.46 (8)
Fe(4)-Fe(3)-C(3B)	165.9 (1)	161.47 (9)
Fe(4)-Fe(3)-C(3C)	78.68 (8)	76.17 (8)
C(5)-Fe(3)-C(3A)	94.6 (1)	92.5 (1)
C(5)-Fe(3)-C(3B)	139.1 (1)	142.6 (1)
C(5)-Fe(3)-C(3C)	122.7 (1)	120.0 (1)
H_b-Fe(3)-C(3A)	178.5 (2)	178.8 (2)
H_b-Fe(3)-C(3B)	82.4 (2)	79.6 (2)
H_b-Fe(3)-C(3C)	84.6 (2)	89.5 (2)
C(3A)-Fe(3)-C(3B)	96.0 (1)	97.5 (1)
C(3A)-Fe(3)-C(3C)	95.6 (1)	95.2 (1)
C(3B)-Fe(3)-C(3C)	95.4 (1)	94.9 (1)
Fe(2)-Fe(4)-C(4A)	149.4 (1)	148.23 (9)
Fe(2)-Fe(4)-C(4B)	100.19 (9)	95.85 (9)
Fe(2)-Fe(4)-C(4C)	108.47 (9)	100.41 (9)
Fe(3)-Fe(4)-C(4A)	97.24 (9)	98.94 (8)
Fe(3)-Fe(4)-C(4B)	151.1 (1)	150.0 (1)
Fe(3)-Fe(4)-C(4C)	108.47 (8)	108.33 (8)
C(5)-Fe(4)-C(4A)	102.5 (1)	100.4 (1)
C(5)-Fe(4)-C(4B)	103.4 (1)	103.8 (1)
C(5)-Fe(4)-C(4C)	150.7 (1)	151.9 (1)
C(4A)-Fe(4)-C(4B)	92.7 (1)	95.5 (1)
C(4A)-Fe(4)-C(4C)	97.3 (1)	97.9 (1)
C(4B)-Fe(4)-C(4C)	97.0 (1)	95.4 (1)
Fe-C-O Bond Angles		
Fe(1)-C(1A)-O(1A)	178.1 (2)	178.9 (2)
Fe(1)-C(1B)-O(1B)	179.1 (2)	179.4 (2)
Fe(1)-C(1C)-O(1C)	178.8 (2)	178.3 (2)
Fe(2)-C(2A)-O(2A)	177.5 (2)	178.9 (2)
Fe(2)-C(2B)-O(2B)	177.7 (2)	175.6 (2)
Fe(2)-C(2C)-O(2C)	174.6 (2)	173.0 (2)
Fe(3)-C(3A)-O(3A)	179.1 (2)	178.3 (2)
Fe(3)-C(3B)-O(3B)	177.5 (2)	176.6 (2)
Fe(3)-C(3C)-O(3C)	173.5 (2)	173.7 (2)
Fe(4)-C(4A)-O(4A)	177.2 (2)	177.7 (2)
Fe(4)-C(4B)-O(4B)	176.5 (2)	177.8 (2)
Fe(4)-C(4C)-O(4C)	178.6 (2)	178.2 (2)

[a] Estimated standard deviations are given in parentheses.

was established for the isoelectronic and isostructural cluster, $HFe_4(\eta^2\text{-}CO)(CO)_{12}^-$ (**2**),[13] where the short distance was 1.81 Å and the others, Fe(1) through Fe(3), were 2.17, 2.10, and 2.10 Å. Thus, the Fe–C distance for the apical iron atom opposite the η^2 ligand appears to be uniformly short. Extended Hückel calculations were made for $HFe_4(\eta^2\text{-}CH)(CO)_{12}$ by using the parameters established in this study and for models of the cluster in which the CH vector was moved away from Fe(1) to Fe(1)–H_a separations of 2.09 and 2.39 Å, respectively.[20] In the last model, the C–H vector was normal to the Fe(1)–Fe(4) vector (because no minimization of energy in the models could be achieved by bond distance variation in our calculational procedure, the results ob-

(20) See R. Hoffmann, *J. Chem. Phys.*, **39**, 1397 (1963), for description of EHMO program. The following parameters were used: atom (orbital, H_{ii} (eV), ζ), H (1s, -13.6, 1.3), C (2s, -21.4, 1.625), C (2p, -11.4, 1.625), O (2s, -32.3, 2.275), O (2p, -14.8, 2.275), Fe (4s, -9.17, 1.90), Fe (4p, -5.37, 1.90), Fe (3d, -12.7, 4.07).

Table V. Selected Intermolecular Contact Distances (Å) and Angles (Deg) for $HFe_4(\eta^2\text{-CH})(CO)_{12}$[a]

		Molecule 1[b]	
H_a-O(3B)^i	2.574 (4)	C(5)-H_a-O(3B)^i	123.1 (3)
Fe(1)-H_a-O(3B)^i	138.1 (2)	H_a-O(3B)^i-C(3B)	142.1 (3)
		Molecule 2	
H_aP-O(4B)P^{ii}	2.485 (5)	H_aP-O(4B)P^{ii}-C(4B)P^{ii}	167.3 (5)
H_bP-O(1A)^{iii}	2.697 (5)	Fe(2)P-H_bP-O(1A)^{iii}	127.3 (2)
Fe(1)P-H_aP-O(4B)P^{ii}	125.9 (2)	Fe(3)P-H_bP-O(1A)^{iii}	118.8 (2)
C(5)P-H_aP-O(4B)P^{ii}	122.6 (3)	H_bP-O(1A)^{iii}-C(1A)^{iii}	173 (1)

[a] Atoms of the second molecule of the asymmetric unit are designated with the letter P. [b] Symmetry operations used: (i) $x, 1/2 - y, 1/2 + z$; (ii) $1 - x, -y, 1 - z$; (iii) $x, 1/2 - y, z - 1/2$.

Table VI. Shape Parameters for Iron Butterfly Structures

		angles, deg		distances, Å		
cluster	structure	δ_w[a]	Fe(1)-C-Fe(4)[b]	Fe(1)-C	Fe(4)-C	Fe(2,3)-C(av)
$HFe_4(\eta^2\text{-CH})(CO)_{12}$[c]	Figures 1 and 2	110.6	170.5 (1)	1.927 (2)	1.827 (2)	1.945 (4)
$[HFe_4(\eta^2\text{-CO})(CO)_{12}^-]$	2	117		2.17	1.81	2.10
$[HFe_4C(CO)_{12}^-]$	3	104	174 (2)	1.795 (5)	1.795 (5)	1.99 (4)
$Fe_4C(CO)_{13}$	4	101	175.9 (2)	1.779 (4)	1.799 (4)	1.993 (4)
$[Fe_4(CCOOCH_3)(CO)_{12}^-]$	5	129.9	147.9 (5)	2.027 (9)	2.012 (9)	1.955 (9)

[a] Dihedral angle between the planes defined by the two basal iron atoms with each of the apical iron atoms. [b] Iron atoms 1 and 4 are the apical iron atoms, and iron(1) is always the iron atom bonded to both atoms of the η^2 ligand in the $Fe_4(\eta^2\text{-xy})L_z$ type of cluster. [c] Molecule 1 as noted in this study.

Chart I

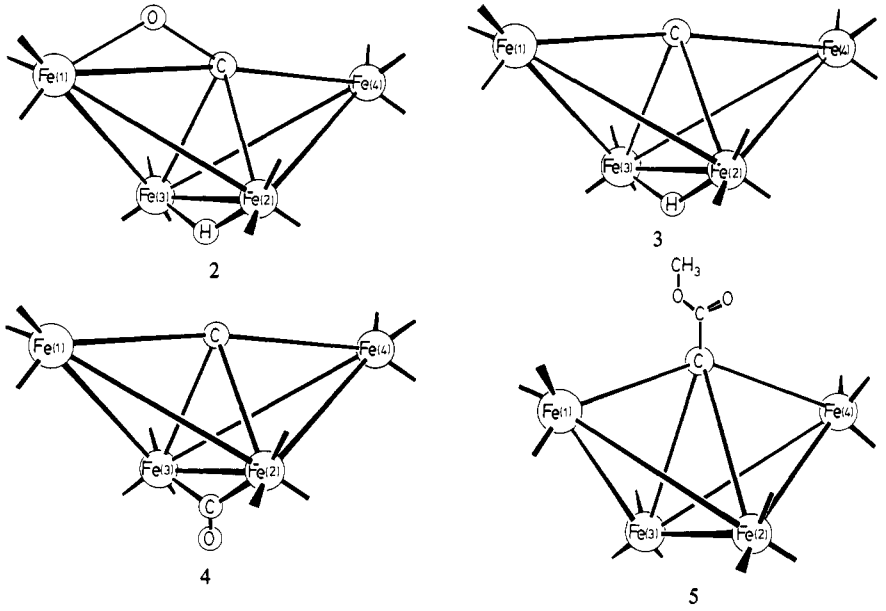

viously must be viewed with caution). Aside from the expected reduction in the overlap population for H_a–Fe(1), the most notable changes were in the populations for C(5)–Fe(1) and C(5)–Fe(4), respectively, which increased and decreased significantly by one order of magnitude in going from the real molecule to the intermediate and 90° C–H models. Qualitatively, within the limits of calculational procedure, the result can be interpreted as follows. As the CH vector is tipped toward apical iron atom, Fe(1), to develop the three-center C–H–Fe interaction observed in the molecule, there is a substantially enhanced carbon p orbital overlap with the other apical iron atom, Fe(4), relative to that of the model in which the C–H vector is normal to the Fe(1)–Fe(4) vector and of course relative to the C(5)-Fe(1) overlap. Mulliken bond orders for the bonds between C(5) and the basal iron atoms, Fe(2) and Fe(3), were not significantly altered by the changes in the CH tilt.

The CO Ligands. Each iron atom in $HFe_4(\eta^2\text{-CH})(CO)_{12}$ is terminally bonded to a set of three carbonyl ligands. The range and the average values for the Fe–C(CO) bonds (molecule 1) are 1.777 (2)–1.835 (2) Å and 1.804 (11) Å, respectively. For both molecules in the asymmetric unit, the Fe–C(CO) bonds centered at Fe(4) appear to be almost significantly different from the rest: the Fe(4)–CO ligand trans to the η^2-CH ligand is long and the other two are short. All C–O bond distances (both molecules) are normal and fall in the narrow range of 1.135–1.155 Å.

The stereochemistry of the CO ligand array about each apical iron atom suggests an octahedral (trigonal) $Fe(CO)_3$ fragment; the vicinal interbond (OC)C–Fe–C(CO) angles are in the range of 92.7 (1)–99.6 (1) Å. Because of the multicenter bonding and the core-compressed character of other atoms interacting with these apical $Fe(CO)_3$ fragments, a discussion of the other interbond angles would serve no purpose. For the basal iron atoms, there is an array of ligand atoms that suggests that each basal iron atom and peripheral ligands form a "C_{2v}" $FeH(CO)_3$ fragment. The bridging hydride hydrogen atom, H_b, is effectively trans to a carbonyl ligand (the angles are 177.6 and 178.5° in molecules 1 and 2, respectively). In these two $FeH(CO)_3$ fragments, the range of (OC)C–Fe–C(CO) angles is 95.1–97.8° and the range of cis H_b–Fe–C(CO) angles is 82.4–87.3°, the latter angles explicably smaller than the former which are based solely on the larger CO ligands. The short Fe-C(CO) bond distances are not trans to the bridging hydride hydrogen atom, H_b. As noted above,

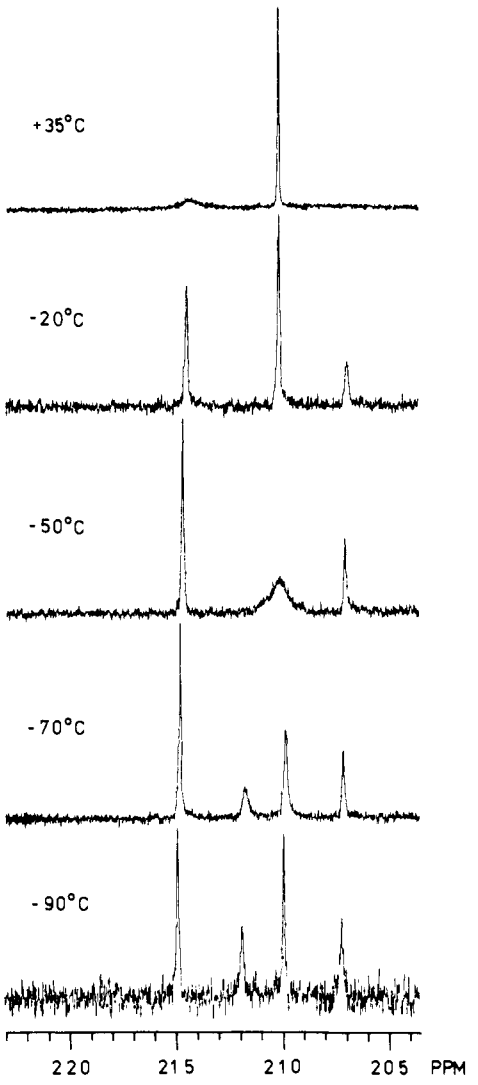

Figure 4. $^{13}C\{^1H\}$ CO DNMR spectra of $HFe_4(CH)(CO)_{12}$ between -90 and +35 °C. The resonance at 215 ppm is a doublet ($J = 7$ Hz) due to the hydride proton when not decoupled. The assignment in the direction of increasing field is δ, β, α, and γ referenced to structure **6**.

the two shortest distances are Fe–CO bonds centered at Fe(4) and are cis to the methylidyne carbon atom; the unique, long bond at Fe(4) is the Fe(4)–C(CO) bond trans to the methylidyne carbon atom. However, these differences in distances are of marginal statistical significance even though the same pattern was observed in both molecules in the asymmetric unit. Carbonyl ligand–ligand repulsions are nicely minimized in the observed CO stereochemistry relative to the Fe_4C core atoms. An analogous conformation appears (based on available data) to prevail in the isoelectronic $[HFe_4(\eta^2\text{-}CO)(CO)_{12}^-]$ cluster.[16]

A number of exchange processes are operative in $HFe_4(\eta^2\text{-}CH)(CO)_{12}$. In addition to the aforementioned hydrogen atom exchange between the C–H–Fe(1) and Fe(2)–H–Fe(3) sites, fast intramolecular CO exchange occurs in the cluster at 20 °C. In Figure 4, the ^{13}C CO DNMR spectra for **1** are presented. At low temperatures, there are only four differentiable ^{13}C resonances of relative intensities 4:2:4:2. In the structure established for the solid state (Figures 1 and 2), there are seven differentiable CO environments. The persistance of only four ^{13}C carbonyl resonances even at −118 °C suggests that some dynamic process is still operative so as to yield on the NMR time scale a molecule of dynamic C_{2v} symmetry. A plausible process is a rapid switch of the CH hydrogen atom between C(5)–H_b–Fe(1) and C(5)–H_b–Fe(4) sites; the precise geometric pathway of the hydrogen atom migration in this site exchange cannot be established from the ^{13}C NMR data.

At temperatures above −90 °C, there are specific CO-exchange processes that become fast on the NMR time scale (Figure 4). The ^{13}C DNMR spectra can be explained by the labeled structure **6**, based on the crystallographic analysis:

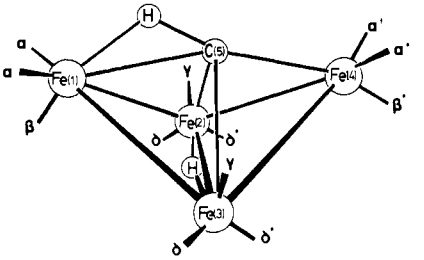

6

(A) at −118 °C, fast CH hydrogen atom switch yields two sets of CO environments (α and β) of ratio 2:1 for CO ligands attached to the apical iron atoms, Fe(1) and Fe(4), and two analogous sets of CO environments (γ and δ) associated with the basal iron atoms; (B) at −70 to −50 °C, intrametal site CO exchange (localized at a single metal atom) becomes fast for the CO ligands at the apical iron sites, Fe(1) and Fe(4); (C) near 0 °C, intrametal site CO exchange occurs at a rate comparable to the NMR time scale for the CO ligands at the basal iron sites, Fe(2) and Fe(3), but the rate is not sufficiently high even at +35 °C to coalesce the γ and δ CO resonances into a single sharp resonance.

Intermetal CO site exchange was not rapid up to +35 °C. The CO-exchange behavior established for $HFe_4(\eta^2\text{-}CH)(CO)_{12}$ appears to be general for the class of $Fe_4X(CO)_{12}^{y-}$ clusters (X = C, $y = 2$;[3] X = N, $y = 1$[21]).

Acknowledgment. This work was performed under the auspices of the Office of Basic Energy Sciences of the U.S. Department of Energy. We also wish to acknowledge the partial support of this collaborative reseach by the National Science Foundation Grant CHE-78-20698 to J.M.W. and E.L.M. and Grant CHE-79-03933 to E.L.M. and the assistance of Mr. David Grier for the EHMO calculations. We also are indebted to J. S. Bradley, D. Shriver, and M. Manassero for providing us with unpublished information about iron butterfly structures.

Supplementary Material Available: A listing of the observed and calculated structure (19 pages). Ordering information is given on any current masthead page.

(21) M. Tachikawa, J. Stein, E. L. Muetterties, R. G. Teller, E. Gerbert, and J. M. Williams, *J. Am. Chem. Soc.*, **102**, 6648 (1980).